PATIENT SPECIFIC AORTIC BLOOD FLOW SIMULATION BASED ON 4D MRI DATA

Romain Lemore | CASIS & COMMEDIA project-team (Inria, Sorbonne université, CNRS)

Joint work with :

Armando Barrera	CASIS - Dijon
Jean-Joseph Christophe	CASIS - Dijon
Miguel A.Fernandez	Sorbonne Université, CNRS, INRIA - Paris
Damiano Lombardi	Sorbonne Université, CNRS, INRIA - Paris
You Zhou	ICMUB - Dijon

Clinical Context

- Some pathologies are correlated with the formation of aneurisms such as Bicuspid Aortic Valves
- Currently the criteria to predict rupture are aneurysm diameter and growth rates.
  - The limitations of these anatomical criteria are well known.
  - Among 591 patients with aortic dissection, [1] found that 59% of them had an aorta diameter below the threshold.
- Some diseases have a major impact on blood flow
  - This can alter the jet angle, which correlates with increased wall shear stress (WSS), a factor responsible for wall thinning.

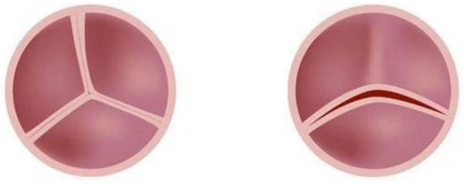

Tricuspid valve and bicuspid valve

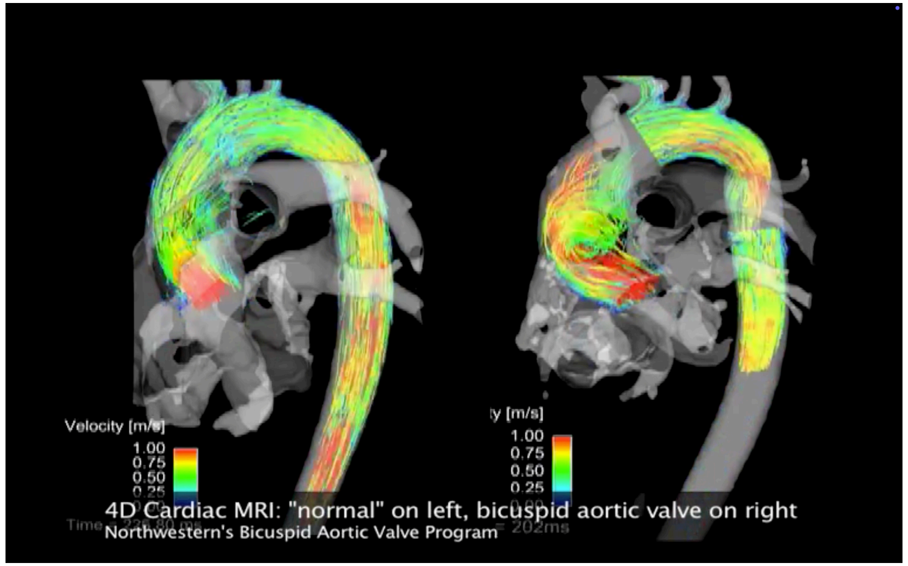

Velocity streamlines from Bluhm Cardiovascular institute
https://www.youtube.com/watch?v=bIULEWqBXeY

[1] **Pape et al. (2007)** Aortic diameter >or = 5.5 cm is not a good predictor of type A aortic dissection: observations from the International Registry of Acute Aortic Dissection (IRAD).

MRI data

- MRI is a **non-invasive** imaging technique used to visualize internal body structures.
  - It relies on the **resonance properties of hydrogen nuclei** when exposed to a strong magnetic field.
- The same technology can be used to **quantify tissue velocity** within each voxel using a **4D flow sequence**.
  - Provides accurate measurement of blood flow rates (relative error < 3.6%).
  - The data is noisy at the voxel level, with relative errors reaching up to 20% [1][2].
  - Spatial resolution is typically around 2 mm × 2 mm × 2 mm.

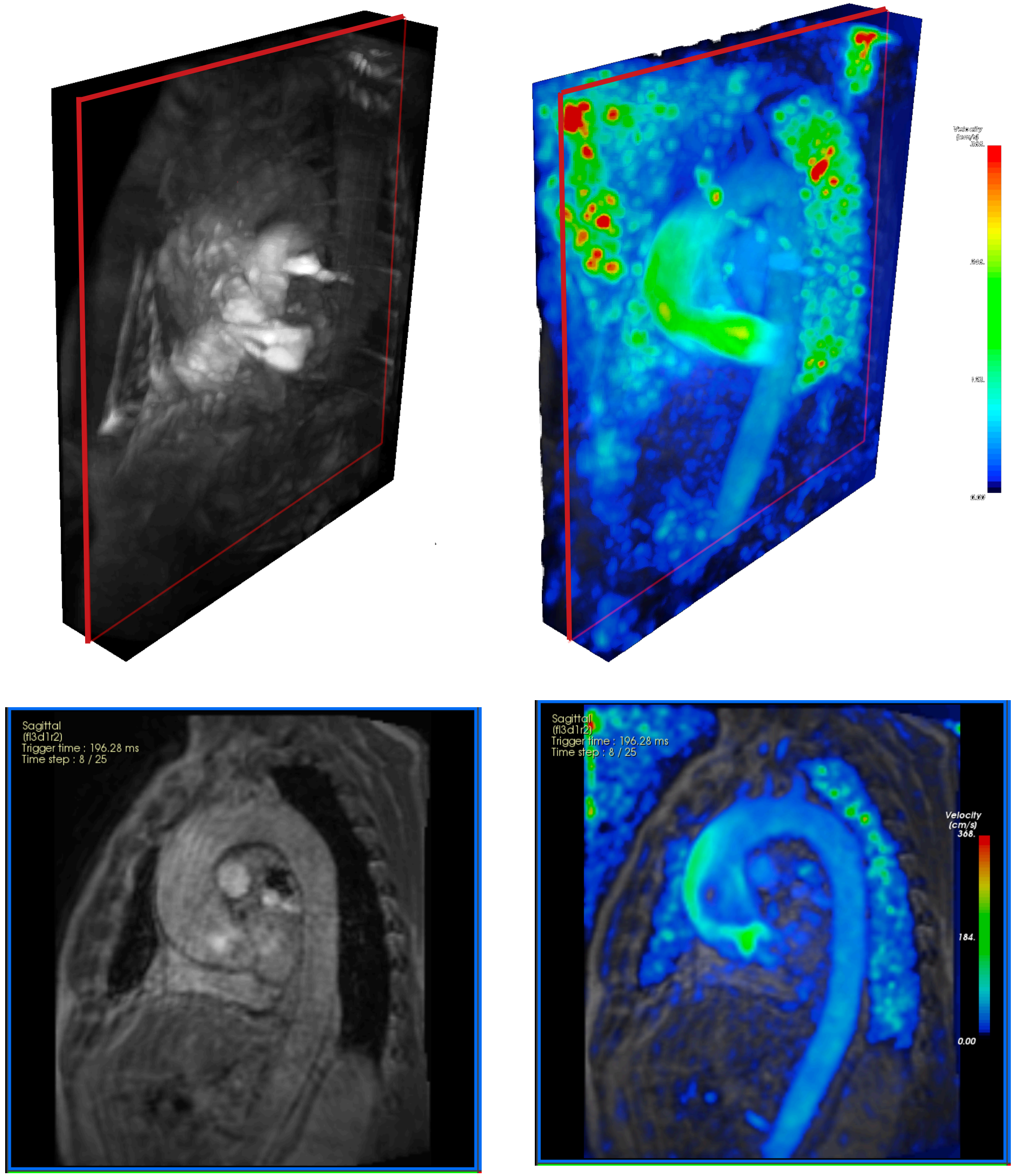

MRI and 4D MRI images

[1] **Kweon J. et al. (2016).** Four-dimensional flow MRI for evaluation of post-stenotic turbulent flow in a phantom: comparison with flowmeter and computational fluid dynamics.
[2] **Töger, Johannes et al. (2015).** Phantom validation of 4D flow: Independent validation of flow velocity quantification using particle imaging velocimetry.

Basic Principles of MRI

- The principle is to align the magnetization vectors of the hydrogen protons with a very strong external magnetic field.

- The precession frequency of the magnetization vector is proportional to the magnetic field strength $\omega = \gamma B_0$.

- By varying the magnetic field with respect to position, the received signal becomes the **Fourier transform** of the longitudinal particles' magnetic moment distribution :

- $$S(k_x, k_y) = \int_\Omega \rho(r)\ e^{-i\gamma \int_t \vec{G}\cdot r} = \int_\Omega \rho(r)\ e^{-2\pi i(k_x x + k_y y)}$$

with

$$k_x = \frac{\gamma t}{2\pi}\int_0^{t'} G_x(t')\ dt' \text{ et } k_y = \frac{\gamma t}{2\pi}\int_0^{t'} G_y(t')\ dt'$$

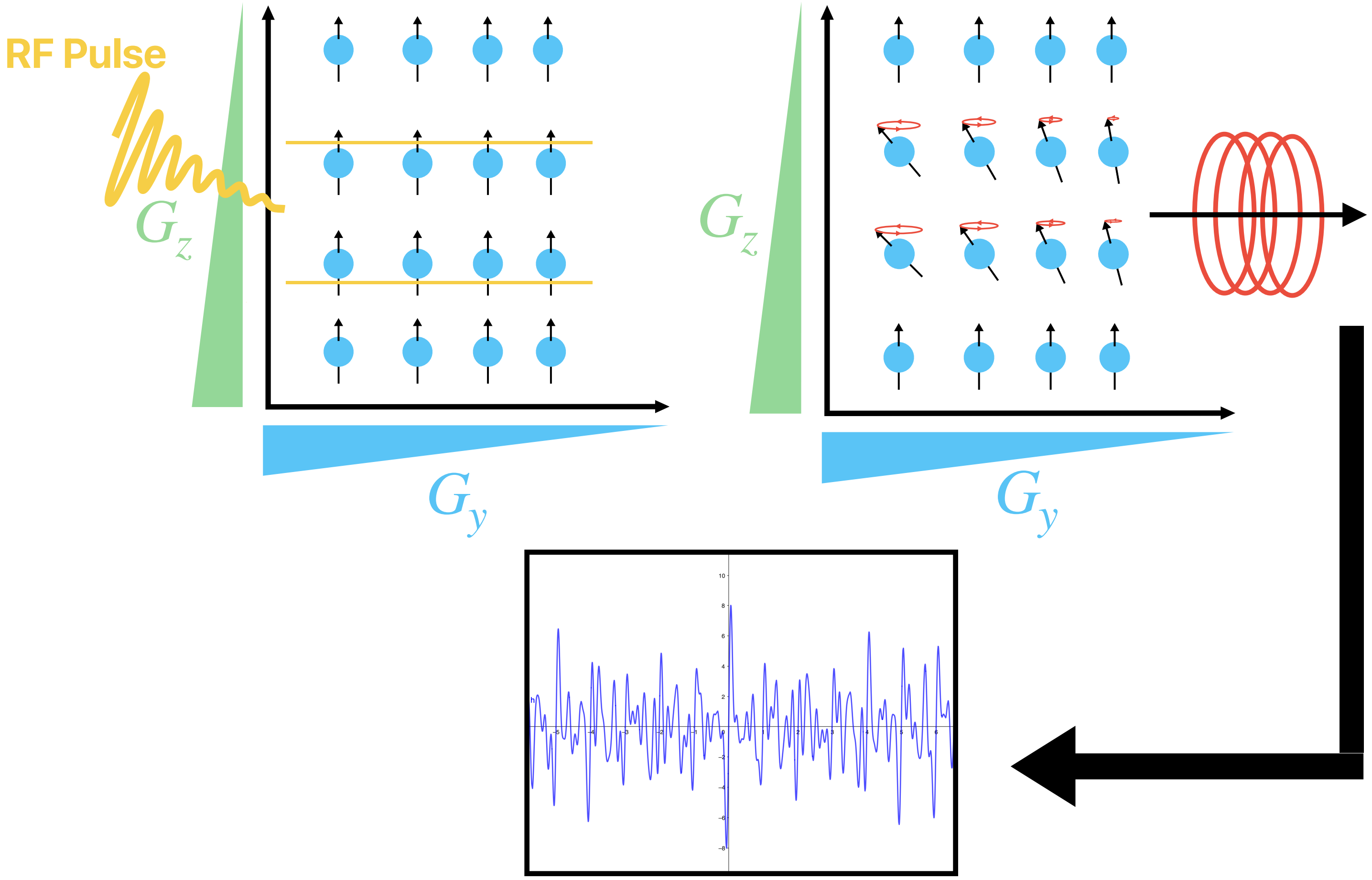

$$S(t) = S(k_x, k_y)$$

Basic Principles of 4D MRI
Velocity estimation

For each velocity component :

- The idea is to track the information transported by a particle.
- Considering $\mathbf{r}(\mathbf{t_0} + \delta \mathbf{t}) = \mathbf{r_0} + \delta t\, \mathbf{v_0} + \mathbf{o}(\delta \mathbf{t})$ we obtain :

$$S(t) = \int_{\Omega} \rho(r)\ e^{-i \int_t \vec{G} \cdot r}$$

$$\int_{t=0}^{\delta t} G(t) r\ dt = \gamma r(0) \cdot \underbrace{\cancel{\int_0^{\delta_t} \vec{G}(t)\ dt}}_{M_0} + \gamma v(0) \underbrace{\int_0^{\delta_t} \delta_t \vec{G}(t)\ dt}_{M_1} + o(\delta_t^2)$$

- The velocity is recovered using two close angle measurement by :

$$v_{x_i} = \frac{v_{ENC}}{\pi} (\phi_1^{[x_i]} - \phi_2^{[x_i]}). \quad \text{with } \phi_j^{[x_i]} = arg(S_j^{[x_i]})$$

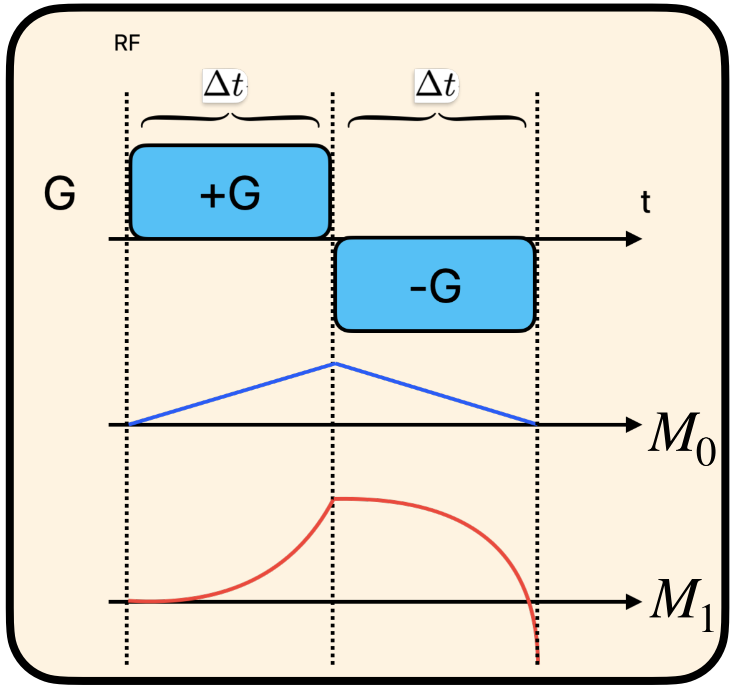

Velocity gradient sequence

Benefits of CFD Models

- Estimating quantities of interest directly from noisy data is challenging, especially when they depend on derivatives of the velocity field like the WSS.
- CFD approach can be a favorable approach
  - Non invasive
  - Easily reproducible
  - Potentially patient-specific
  - Overcomes limitations due to noisy data
  - Provides access to markers that are difficult to measure in vivo (e.g., pressure estimation)

WSS corresponds to the tangential component of the stress vector at each point on the surface .

$$\sigma \vec{n} \cdot \tau$$

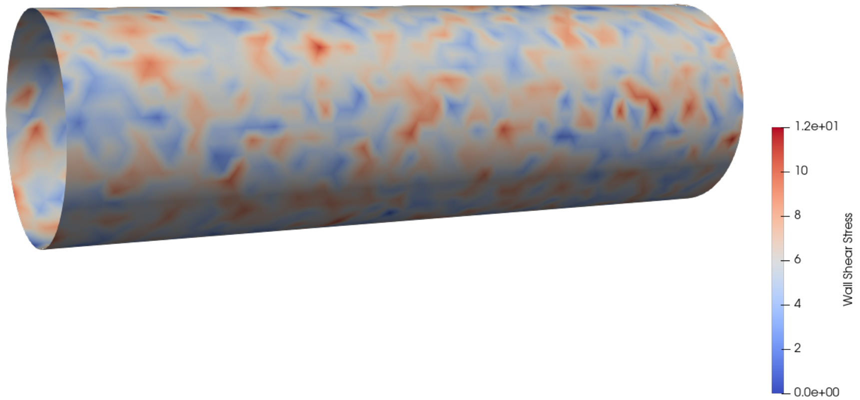

WSS computed directly from an analytical Poiseuille flow which has been noised.
The target value is 6.1 Pa

Existing approaches

- Several studies have address this problem by considering direct approach.
- Direct approach presents several limitations.
  - Imposing accurate inlet boundary conditions is difficult because of noise in the measurements.
  - At the outlet, a 0D model must be carefully calibrated [1][2].
    - It can be calibrated manually as in
      Mollo, Pierre et al. (2025). *Accurate Cerebral Blood Flow Simulations Compared to Real Data. Mathematical Modelling of Natural Phenomena.*
    - Or Automatically as proposed in
      Arthurs CJ et al (2020). *A flexible framework for sequential estimation of model parameters in computational hemodynamics.*
- To address these challenges, we propose an inverse modeling approach based on 4D-MRI data.

$(u,p) \in (H^1, L_2^0)$ solves the following problem :

$$\begin{cases} \dfrac{\partial u}{\partial t} + u\nabla u - \Delta u + \nabla p = 0 & \text{in } \Omega \\ div(u) = 0 & \text{in } \Omega \\ u = u_{IRM} & \text{on } \Gamma_{\text{Inlet}} \\ u = 0 & \text{on } \Gamma_{\text{Wall}} \\ \sigma \vec{n} = RQ\vec{n} & \text{on } \Gamma_{\text{Outlet}} \end{cases}$$

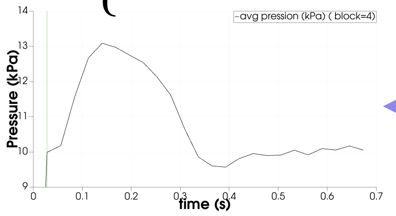

Pressure in the aortic branch

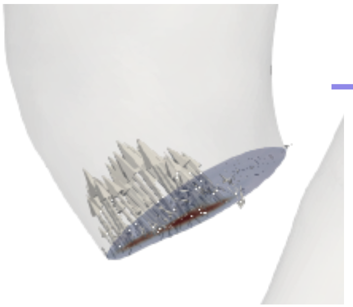

Inlet Boundary condition

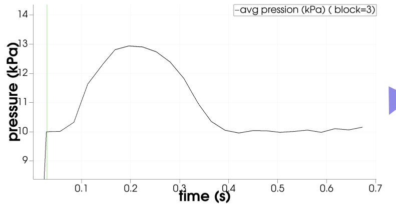

Pressure in the descending aorta

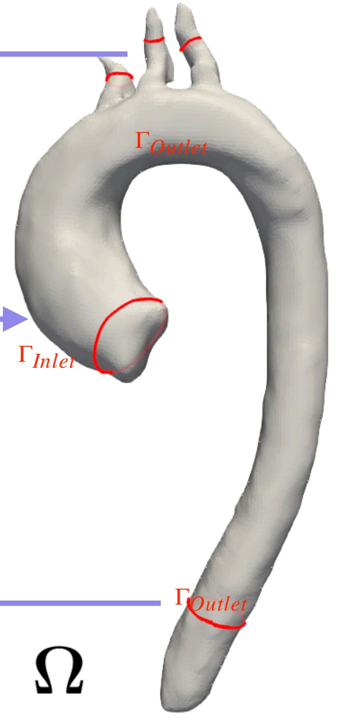

Aorta mesh with his boundary slices

Selected approach

- The idea is to **incorporate data over the entire domain** to compensate for the lack of boundary conditions.
- Time steps are treated independently, in order to avoid solving large coupled systems.

$$\min_{\mathscr{M}(u)=0} \frac{1}{2} \int_{t=t_0}^{T_N} \int_{\Omega} \| \, u - u_{meas} \, \|^2 \; dV \, dt \quad \longrightarrow \quad \min_{\mathscr{M}(u^{n+1}, u^n)=0} \int_{\Omega} \| \, u^{n+1} - u_{meas} \, \|^2 \; dV$$

- The resulting problem is **ill-posed** and requires proper stabilisation.
- We propose an approach where we **discretize the problem first**, and then apply **regularization**.
  - The method is **weakly consistent**.
  - Allows a **convergence estimate.**

Inverse Problem Formulation

- This work is based on the results of the following work :
  - ***Boulakia, Muriel & Burman, Erik & Fernández, Miguel & Voisembert, Colette. (2020).*** *Data assimilation finite element method for the linearized Navier–Stokes equations in the low Reynolds regime. Inverse Problems.*
- This work is done on a stationary framework.
- The idea here is to explore the transient case.
- This approach allows us to compensate the lack of boundary conditions by the data.
- $\| \cdot \|_\gamma$ reflects the relative confidence assigned to the data (for exemple $\gamma \| \cdot \|_{L_2}$)

$$\min_{\mathcal{M}(u)=0} \| u - u_{meas} \|_\gamma^2$$

$$\mathcal{M}(u) = \begin{cases} \dfrac{\partial u}{\partial t} + u \nabla u - \Delta u + \nabla p - f \\ div(u) \end{cases}$$

Inverse Problem Formulation
Time discretization

Temporal semi-implicit discretization

Let $u^n \in H^1$ and $p^n \in L_0^2$

$$\min_{\substack{NS(u^{n+1})=f \\ div(u)=0}} \| u^{n+1} - u^{n+1}_{meas} \|^2_\gamma$$

$$NS(u^{n+1}) = \frac{u^{n+1} - u^n}{\delta_t} + u^n \nabla u^{n+1} - \Delta u^{n+1} + \nabla p^{n+1}$$

Let $u^n \in H^1$, $p^n \in L_0^2$ and $v \in H_0^1$ and $q \in L^2$

Variational formulation : $NS([u^{n+1}, p^{n+1}], [v, q])$ =

$$\underbrace{\underbrace{\langle \frac{u^{n+1}}{\delta t}, v\rangle + \langle u^n \nabla u^{n+1}, v\rangle + \langle \varepsilon(u^{n+1}), \varepsilon(v)\rangle}_{a(u^{n+1}, v)} - \underbrace{\langle p^{n+1}, div(v)\rangle + \langle q, div(u^{n+1})\rangle}_{-b(p^{n+1}, v) + b(q^{n+1}, u)}}_{A[(u^{n+1}, p^{n+1}), (v, q)]} = \langle f^{n+1}, v\rangle + \langle \frac{u^n}{\delta t}, v\rangle$$

Inverse Problem Formulation

We then discretize the problem using the finite element method

Stabilisation :

$$\mathscr{L} = \frac{1}{2} \parallel u_h - u_{meas} \parallel_\gamma^2 + A[(u_h, p_h), (v, q)] - \langle f, v \rangle + \frac{1}{2} S[(u_h, p_h), (u_h, p_h)] - \frac{1}{2} S^*[(v, q), (v, q)]$$

Stabilisation termes

$$S[(u_h, p_h), (u_h, p_h)] = s_u(u_h, v_h) + s_p(p_h, q_h)$$

$$S^*[(u, p), (v, q)] = s_u^*(u_h, v_h) + s_p^*(p_h, q_h)$$

$$s_u(u, v) = \sum_{F \in \mathscr{F}_i} \int_F h_F [[\nabla u]][[\nabla v]] + \gamma_{div} \int_\Omega div(u) div(v)$$

$$s_u^*(u, v) = \gamma_u^* \int_\Omega \nabla u : \nabla v$$

$$s_p(p, q) = \gamma_p \int_\Omega h^2 \nabla p \cdot \nabla q$$

$$s_p^*(p, q) = \gamma_p^* \int_\Omega pq$$

[1] **Boulakia, Muriel et al. (2020).** Data assimilation finite element method for the linearized Navier–Stokes equations in the low Reynolds regime. Inverse Problems.
[2] **Burman, Erik. (2016)**. Stabilised Finite Element Methods for Ill-Posed Problems with Conditional Stability.

Inverse Problem Formulation

The optimality system to be solved is therefore the following:

$$\text{find } (u_h, p_h) \in V_h \times Q_h^0 \text{ and } (v_h, q_h) \in V_h \times Q_h^0$$
$$\forall (w_h, x_h) \in W_h \times Q_h \text{and } (y_h, z_h) \in V_h \times Q_h^0$$

$$\begin{cases} A[(u_h, p_h), (w_h, x_h)] - S^*[(v_h, q_h), (w_h, x_h)] = \langle f, w_h \rangle \\ A[(y_h, z_h), (v_h, q_h)] + S[(u_h, p_h), (y_h, z_h)] + \langle u_h, y_h \rangle_\gamma = \langle u_{meas}, y_h \rangle_\gamma \end{cases}$$

In the **stationary** case, we obtain the following results [1] :

Consistency :

- $A[(u - uh, p - ph), (wh, xh)] = - S^*[(zh, yh), (wh, xh)]$

Convergence :

Let $(u, p) \in [H^2(\Omega)]^d \times H^1(\Omega)$ and $(u_h, p_h) \in V_h \times Q_h^0$ et $(z_h, y_h) \in W_h \times Q_h$ solution of the inverse problem, then $\forall \omega_T \subset\subset \Omega$ et $\exists \tau \in (0,1)$

- $|u - u_h|_{\omega_T} \leq Ch^\tau(\| u \|_{[H^2(\Omega)]^d} + \| p \|_{H^1(\Omega)} + h^{-1} \| \delta u \|_{L^2(\omega_M)}) + h \| f \|_{L^2}$

[1] **Boulakia, Muriel et al. (2020).** Data assimilation finite element method for the linearized Navier–Stokes equations in the low Reynolds regime. Inverse Problems.

Inverse Problem Formulation

- The noise in MRI is spatially non-uniform, it depend on the MRI magnitude.
- We need to take its variance into account in the model.
  - The idea is to define the norm as $\| u \|_\gamma = u^T C^{-1} u$ with $C = \mathrm{Cov}(u_{meas})$
- Depending on the MRI acquisition technique, the noise can be either:
  - Directionally independent
  - Coupled across spatial components.

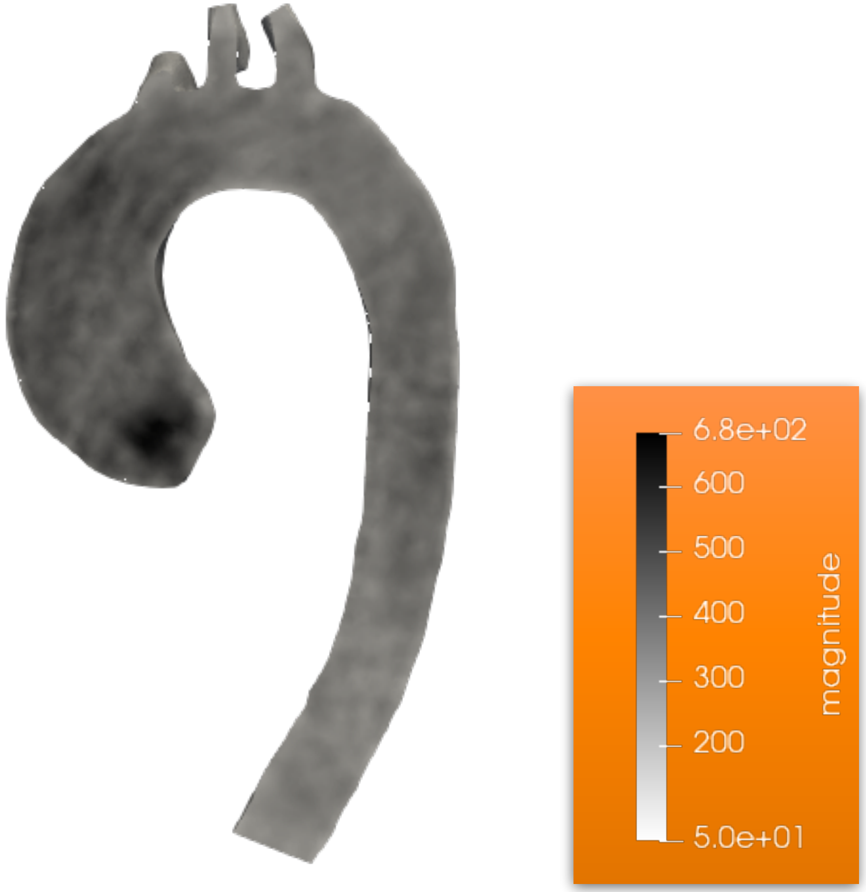

Magnitude at the systolic peak

Recover the velocity covariance matrix

- The covariance matrix will be used to define the weighted norm as follows:

$$\| u \|_\gamma = u^T C^{-1} u$$

- Recall that :

$$v_{x_i} = \frac{v_{ENC}}{\pi}(\phi_1^{[x_i]} - \phi_2^{[x_i]}).$$

- Assuming additive Gaussian[1] noise of equal variance σ^2 , we can derive the variance of ϕ :

$$\sigma^2(\phi) = \frac{\sigma^2(\varepsilon)}{Im^2 + Re^2}$$

- Depending on the acquisition sequence used, we can derive :

$$\begin{cases} v_{x_i} = \dfrac{v_{ENC}}{\pi}(\phi_1^{[x_i]} - \phi_2^{[x_i]}) \\ \text{Then} \\ \text{Cov}(v) = \dfrac{v_{ENC}^2 \; \sigma^2(\varepsilon)}{\pi^2(Im^2 + Re^2)} \begin{pmatrix} 2 & 0 & 0 \\ 0 & 2 & 0 \\ 0 & 0 & 2 \end{pmatrix} \end{cases}$$

$$\begin{cases} v_{x_i} = \dfrac{v_{ENC}}{\pi}(\phi_1^{[Ref]} - \phi_2^{[x_i]}) \\ \text{Then} \\ \text{Cov}(v) = \dfrac{v_{ENC}^2 \; \sigma^2(\varepsilon)}{\pi^2(Im^2 + Re^2)} \begin{pmatrix} 2 & 1 & 1 \\ 1 & 2 & 1 \\ 1 & 1 & 2 \end{pmatrix} \end{cases}$$

[1] **Conturo TE, Smith GD. (1990).** Signal-to-noise in phase angle reconstruction: dynamic range extension using phase reference offsets.

Numerical Results

Time	0.11s			0.17s		
4D MRI data	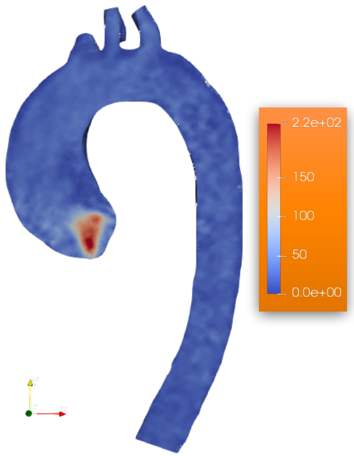			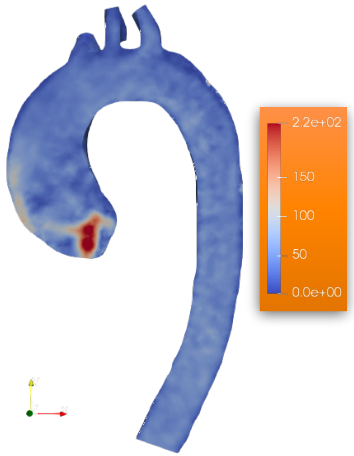		
Comparison of simulations	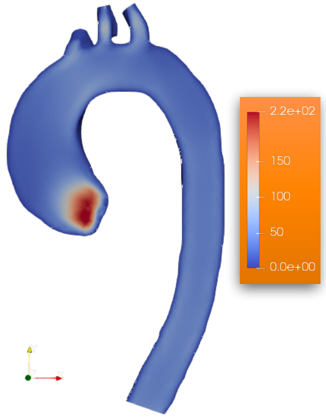	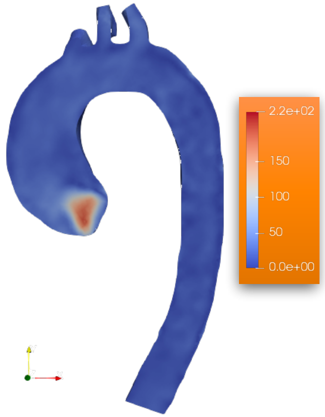	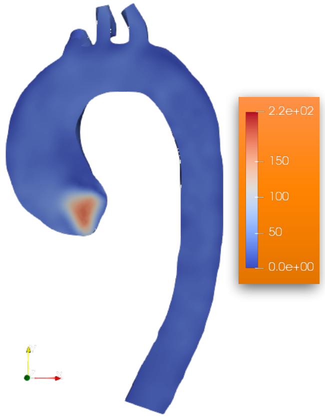	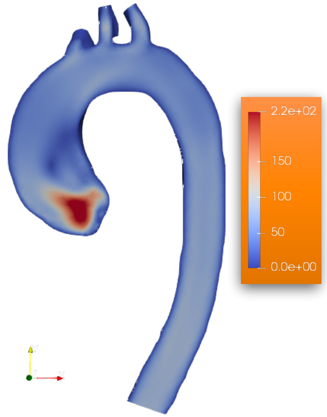	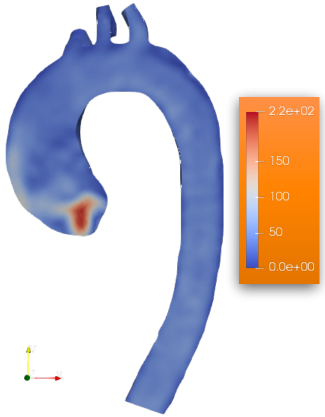	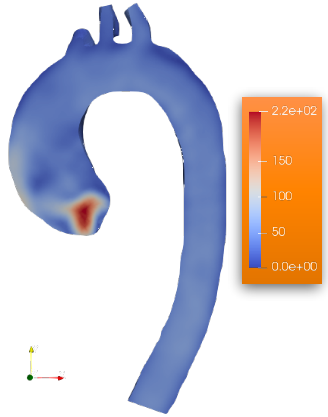
	Direct simulation	U.C with $\| \cdot \|_\gamma = 10^5 \| \cdot \|$	U.C with Coil variance : $1.3 \cdot 10^{-4}$	Direct simulation	U.C with $\| \cdot \|_\gamma = 10^5 \| \cdot \|$	U.C with Coil variance : $1.3 \cdot 10^{-4}$

Discrepancy

	0.11 s	0.17 s	0.22 s
Direct simulation	540.1	748.5	751.0
Unique continuation with $\|\cdot\|_\gamma = 10^5 \|\cdot\|$	272.2	314.9	309.32
Unique continuation with Coil variance : $1.3 \cdot 10^{-4}$	277.86	350.38	347.29

Numerical Results | comparison of pressure estimates at $t = 0.11$

Direct method Simulation	Constant Weight 10^5	Using covariance matrix Coil variance : $6 \cdot 10^{-5}$	Using covariance matrix Coil variance : $1.3 \cdot 10^{-4}$
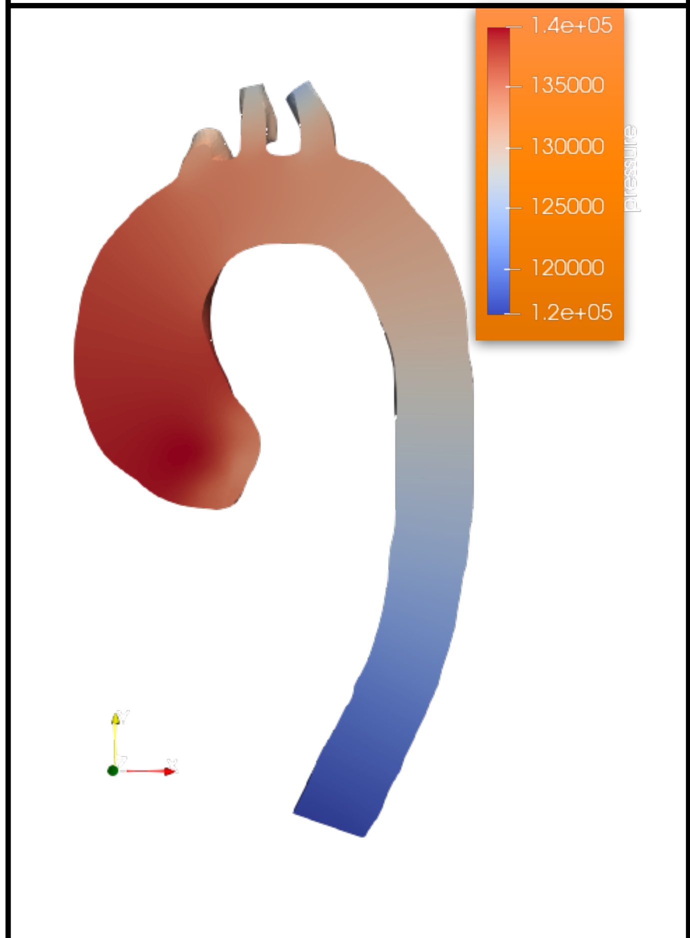	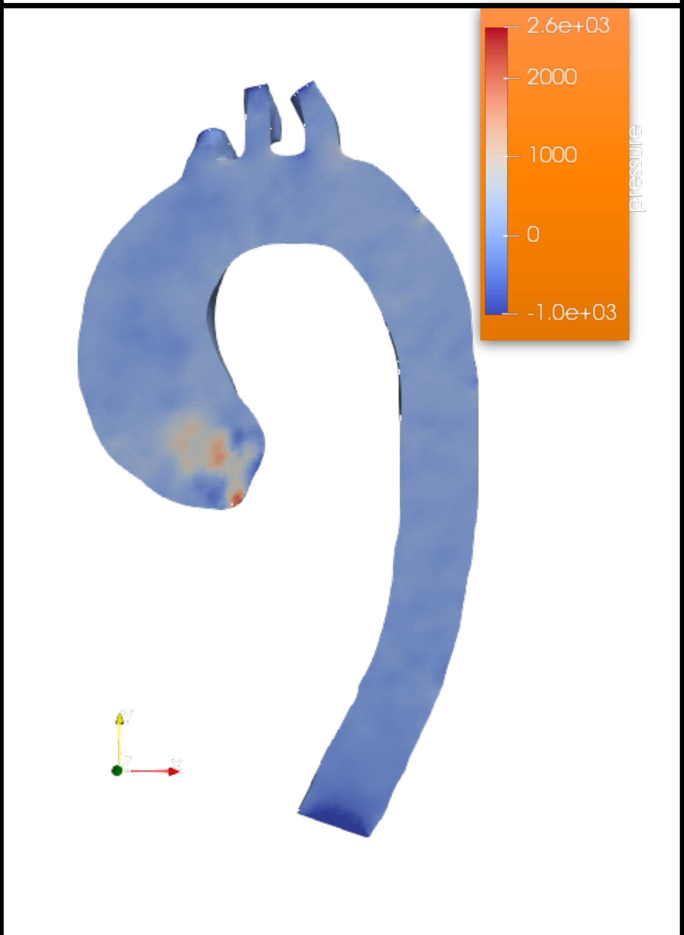	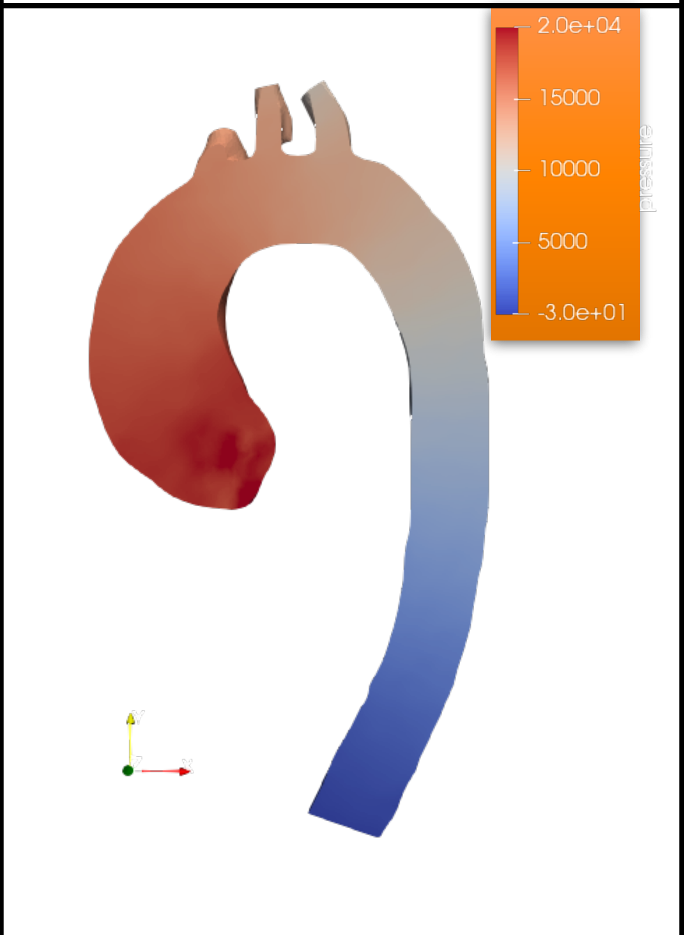	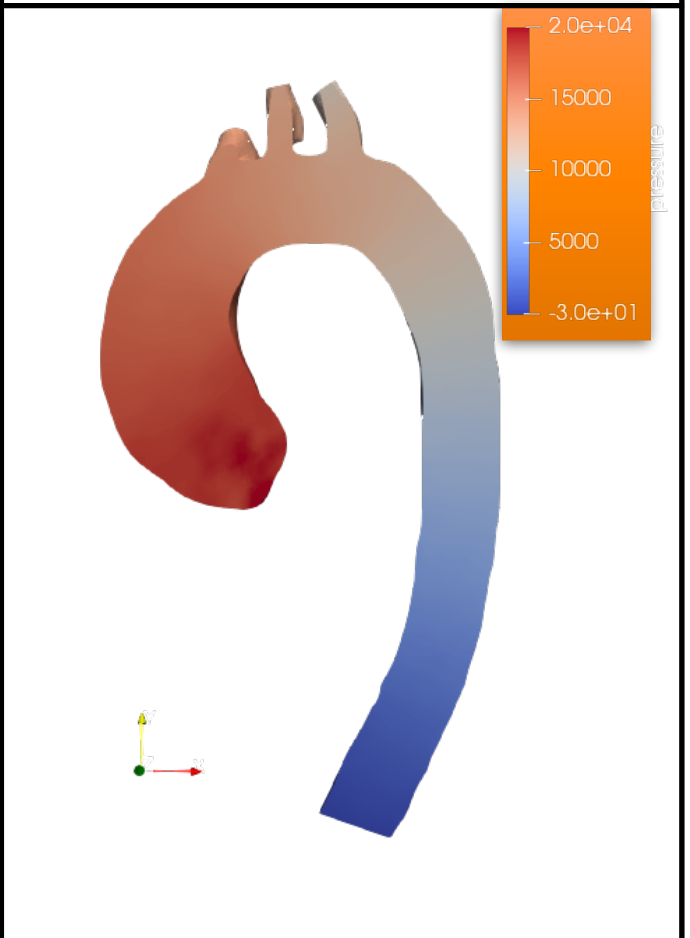

WSS estimation

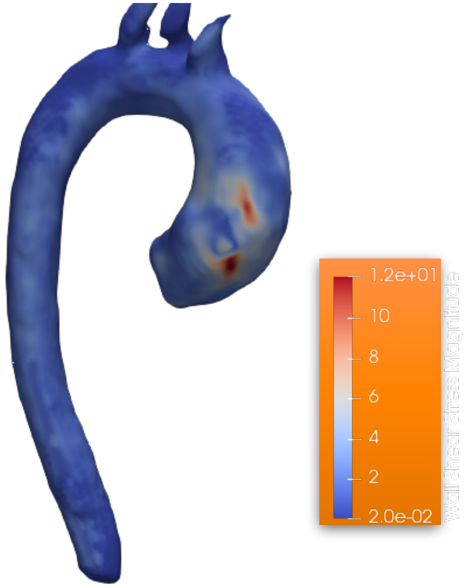

WSS computed directly from the data

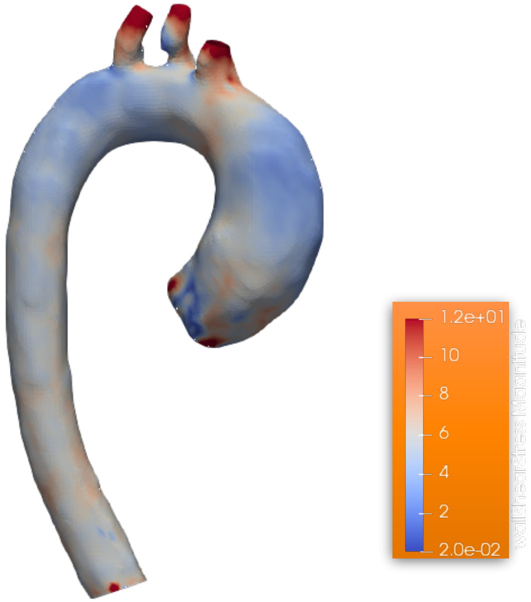

WSS computed from direct simulation

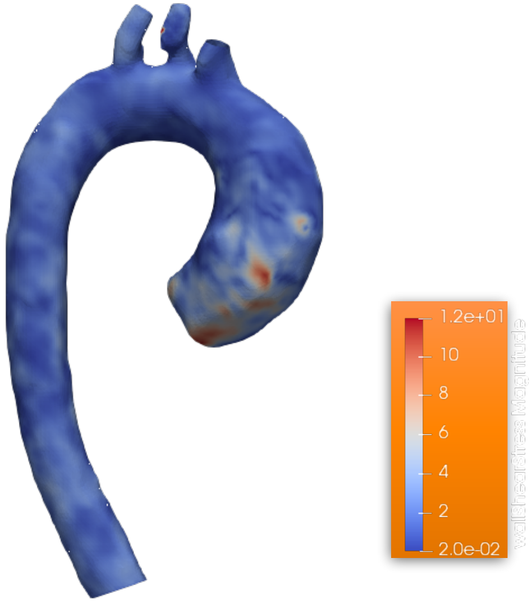

WSS computed from U.C with constant weight

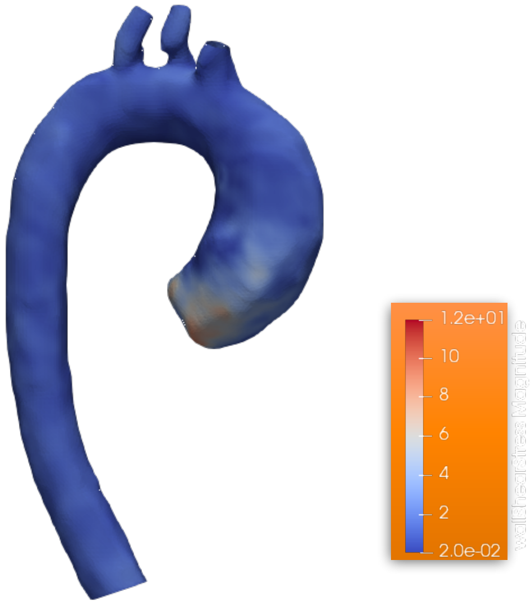

WSS computed from U.C using covariance matrix

Coil variance : $1.3 \cdot 10^{-4}$

Limitations and Perspectives

- The problem we are solving is two times larger
- The wall motion is neglected
- Does the error introduced in the time-dependent problem remain controlled ?

- We are expecting to receive a phantom to experimentally validate our results.
- We also plan to simulate the MRI acquisition process in order to generate realistic synthetic data.

Thank you for your attention.